GAIN-MARGINS AND PHASE-MARGINS OF MULTIVARIABLE TIME-DELAY SYSTEMS

Tsung-Huang Ma
Department of Electrical Engineering, Yuan Ze University, Taiwan, R.O.C

Chih-Min Lin
Department of Electrical Engineering, Yuan Ze University, Taiwan, R.O.C, cml@saturn.yzu.edu.tw

Fei Chao
Cognitive Science Department, School of Information Science and Engineering, Xiamen University, China

Chun-Fei Hsu
Department of Electrical Engineering, Tamkang University, Taiwan, R.O.C

Jih-Gau Juang
Department of Communication and Navigation, National Taiwan Ocean University, Taiwan, R.O.C

See next page for additional authors

GAIN-MARGINS AND PHASE-MARGINS OF MULTIVARIABLE TIME-DELAY SYSTEMS

Authors

Tsung-Huang Ma, Chih-Min Lin, Fei Chao, Chun-Fei Hsu, Jih-Gau Juang, and Ching-Hung Lee

GAIN-MARGINS AND PHASE-MARGINS OF MULTIVARIABLE TIME-DELAY SYSTEMS

Tsung-Huang Ma[1], Chih-Min Lin[1], Fei Chao[2], Chun-Fei Hsu[3],

Jih-Gau Juang[4], and Ching-Hung Lee[5]

ABSTRACT

In this paper, the gain-phase-margin tester method is applied to analyze the gain-margins (GMs) and phase-margins (PMs) of multi-input multi-output (MIMO) control systems with time-delays. The objectives of the proposed method are: (1) to present the basic definitions and physical meanings of GMs and PMs of MIMO control systems; (2) to give some important remarks on how to construct proper block diagrams for those systems originally expressed by state equations; (3) to analyze the GMs and PMs of a missile autopilot system. The analysis results are checked by the use of Nyquist plots and computer simulations.

I. INTRODUCTION

Stability analysis of multi-input-multi-output (MIMO) time delayed systems has been presented in literatures (Liu, 2013; Liu, 2013); however, they didn't take into consideration of the quantitative stabil ity margins such as gain-margins and phase-margins. For the design of industrial control systems, gain-margins (GMs) and phase-margins (PMs) are the two important specifications. Control systems designed with proper values of gain-margins and phase-margins in frequency domain can achieve desirable responses in time domain. In addition, these two margins are also the indications of robust characteristics (Wang et al., 2003; Parakevopoulos et al., 2006; Liceaga-Castro et al., 2012; Wang 2012; Li, 2013) . In general, the specifications

of these two margins must be met no matter what other specifications (such as minimization of the integral of squared error) are used for design.

For single-input single-output (SISO) systems, standard methods are available for finding gain-margins and phase-margins. But, for multi-input multi-output (MIMO) systems, since the physical meanings of these margins are not clearly defined as for SISO systems, there are still some doubts in current literature about whether it is reliable to use gain-margins (GMs) and phase-margins (PMs) as design criteria, especially when the robust characteristics due to parameter variations are considered. Therefore, in the first part of this paper, the physical meanings of GMs and PMs for MIMO systems are presented.

Methods of plotting the boundaries of constant gain-margins and phase-margins in a parameter plane or a parameter space have been proposed for analysis and design of SISO control systems (Chang and Han, 1989, 1990; Shenton and Shafiei, 1994). The extension of the aforementioned results to MIMO control system has been developed (Tao et al., 1991; Li et al., 1993). In these designs, the gain-margins and phase-margins of the MIMO control systems are based upon the augmented open-loop transfer function which is affected by each open feedback of the system. For control systems originally expressed by time domain models, in order to apply the gain-phase-margin tester method, the s-domain models (block diagrams) must be obtained first (Perng et al., 2006). Although any block diagram converted from a time-domain model can be used to find the GMs and PMs, one cannot make sure whether they are the actually required GMs and PMs of the physical system, because this kind of conversion is not unique. Therefore, the second part of this paper is to show how to construct the required structure of the block diagram converted from a time-domain model. For illustration, a missile autopilot system with time delays is analyzed in the final part of this paper.

II. GAIN-MARGINS AND PHASE-MARGINS USING GAIN-PHASE-MARGIN TESTER

In this section, the basic definitions of GM and PM are given as follows (Li et al., 1993):
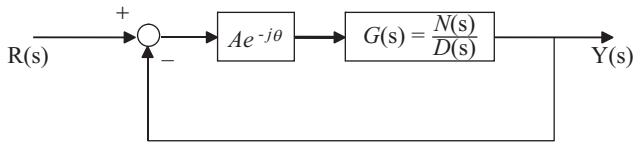
Fig. 1. Block diagram of a system with unity-feedback.

Gain-margin (GM): The amount of increase (denoted by "+") or decrease (denoted by "−") of gain which will make an originally stable system on its stability limit.
Phase-margin (PM): The amount of increase (denoted by "+") or decrease (denoted by "−") of phase-lag which will make an originally stable system on its stability limit.

Gain-phase-margin tester method (Chang and Han, 1989, 1990; Perng et al., 2006):

Consider a feedback system shown in Fig. 1, where $Ae^{-j\theta}$ is the gain-phase-margin tester and $G(s) = \dfrac{N(s)}{D(s)}$ is the open loop transfer function, then the characteristic equation of this system can be expressed as

$$1 + Ae^{-j\theta}G(s)$$
$$= 1 + Ae^{-j\theta}\frac{N(s)}{D(s)} \quad (1)$$
$$= 0,$$

which is equivalent to

$$f(s) \triangleq D(s) + Ae^{-j\theta}N(s) = 0, \quad (2)$$

Let $s = j\omega$, one has

$$f(j\omega) = f(A, \theta, j\omega) = D(j\omega) + Ae^{-j\theta}N(j\omega) = 0, \quad (3)$$

Let $\theta = 0°$; (3) is rearranged as follows.

$$f(j\omega) = f(A, \theta, j\omega) = E \cdot A + F = 0 \quad (4)$$

where E and F are functions of θ and ω, and they are assumed to be known as the open loop transfer function $G(s) = \dfrac{N(s)}{D(s)}$ is given.

Partitioning (4) into real and imaginary parts yields

$$f_R(A, \theta, j\omega) = E_1 \cdot A + F_1 = 0, \quad (5)$$

and

$$f_I(A, \theta, j\omega) = E_2 \cdot A + F_2 = 0, \quad (6)$$

where E_1, E_2, F_1 and F_2 are functions of θ and ω.

Thus, A can be determined directly from (5) and (6), which yield

$$A = \frac{-F_1}{E_1} \triangleq A' \quad (7)$$

and,

$$A = \frac{-F_2}{E_2} \triangleq A''. \quad (8)$$

If $A' = A'' = A_i$, the value of A_i and its corresponding frequency ω_i can be found. For many values of ω, a set (GM) of desired values of A can be obtained. Alternatively, let $A = 0$ dB; (3) is rearranged as follows.

$$f(j\omega) = f(A, \theta, j\omega)$$
$$= U \cdot \cos\theta + V \cdot \sin\theta + W \quad (9)$$
$$= 0$$

where U, V and W are functions of A and ω, and they are assumed to be known as the open loop transfer function $G(s) = \dfrac{N(s)}{D(s)}$ is given.

Also partitioning (9) into real and imaginary parts yields

$$f_R(A, \theta, j\omega) = U_1 \cdot \cos\theta + V_1 \cdot \sin\theta + W_1 = 0 \quad (10)$$

and

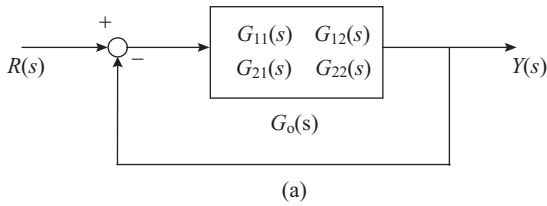$$f_I(A, \theta, j\omega) = U_2 \cdot \cos\theta + V_2 \cdot \sin\theta + W_2 = 0, \quad (11)$$

where U_1, V_1, W_1, U_2, V_2, and W_2 are functions of A and ω. Hence, θ can be determined directly from (10) and (11), which yield

$$\theta = \cos^{-1}(\frac{V_1 \cdot W_2 - V_2 \cdot W_1}{U_1 \cdot V_2 - U_2 \cdot V_1}) \triangleq \theta' \quad (12)$$
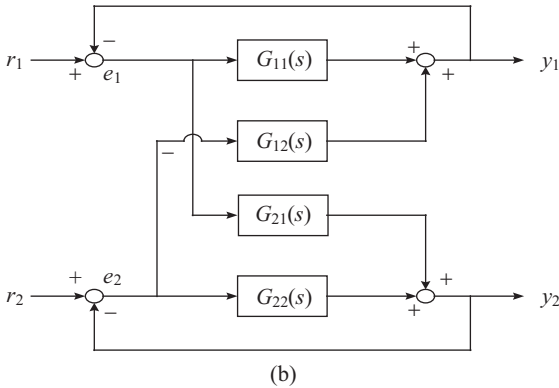
and

$$\theta = \sin^{-1}(\frac{U_1 \cdot W_2 - U_2 \cdot W_1}{U_1 \cdot V_2 - U_2 \cdot V_1}) \triangleq \theta''. \quad (13)$$

If $\theta' = \theta'' = \theta_i$, the value of θ_i and its corresponding frequency ω_i can be found. For many values of ω, a set (PM) of desired values for θ can be obtained.

(a)

(b)

Fig. 2. Block diagram of a MIMO system with unity-feedback.

Fig. 3. The block diagram of a missile autopilot system.

III. BASIC DEFINITIONS AND PHYSICAL MEANINGS OF GAIN-MARGINS AND PHASE-MARGINS OF MIMO SYSTEMS

Consider a MIMO system shown in Fig. 2. By use of the basic concept of gain-phase-margin tester method, the following four kinds of GM and PM are defined.

1. Single-Block GM and PM

Assuming that a gain-phase-margin tester ($Ae^{-j\theta}$) is added in cascade to any single block (G_{ij}) of the system as shown in Fig. 2(b), the physical meaning of single-block GM (PM) is that, the permissible amount of change of gain (phase) of a specific block before the system becomes unstable. In other words, single-block GM and PM are the indications of robust characteristics of the system due to the variations of a pre-specified block.

2. Multi-Block GM and PM

After two or more than two blocks in Fig. 2(b) are added simultaneously with the same gain-phase-margin testers ($Ae^{-j\theta}$, $A_i = A$, $\theta_i = \theta$), the physical meaning of multi-block GM (PM) is that the permissible amount of simultaneous changes of gains (phases) of all the considered blocks before the system becomes unstable.

3. Simultaneous GM an PM

In Fig. 2(b), if every block is added simultaneously with the same gain-phase-margin tester, the physical meaning of simultaneous GM (PM) is that, the permissible amount of simultaneous changes of gains (phases) of all the blocks before the system becomes unstable.
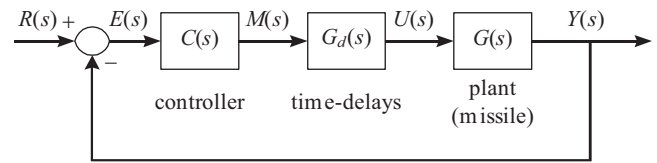
4. Augmented Open-Loop Transfer Function GM and PM

After the matrix $G_0(s)$ is pre-multiplied by a diagonal matrix (L) with gain phase- margin tester ($Ae^{-j\theta}$, $i = 1, 2$) as its elements, if the system is on its stability limit, then $A_i(\theta_i)$ are the augmented open-loop transfer-function (AOLTF) GMs (PMs). This kind of GMs and PMs, which has been analyzed in (Tao et al., 1991; Li et al., 1993), can be regarded as the direct extension of the concept of GM and PM for SISO systems to MIMO systems. In fact, this is a special kind of multi-block GMs and PMs.

From the GMs and PMs defined above, it can be seen that a proper structure of the block diagram must be defined first; then the GMs and PMs of a system can be analyzed.

IV. ANALYSIS OF GM AND PM OF A MISSILE AUTOPILOT SYSTEM EXPRESSED BY TIME-DOMAIN MODEL

A two-input-two-output missile autopilot system had been analyzed by using the principal gain and principal phase method (Postletheaite et al., 1981). Here the same system but with some time-delays is considered. The general block diagram of the system is shown in Fig. 3, where the dynamic equations of the missile are (Postletheaite et al., 1981)

$$\dot{X}_m = A_m X_m + B_m u_m$$
$$\dot{Y}_m = C_m X_m \tag{14}$$

where

$$A_m = \begin{bmatrix} 3.23 & 20 & -476 & 0 & 228 & 0 & 0 & 0 \\ -20 & -3.23 & 0 & 476 & 0 & -228 & 0 & 0 \\ 0.39 & 0 & -1.93 & -16 & -415 & 0 & 0 & 0 \\ 0 & -0.39 & 16 & -1.93 & 0 & -415 & 0 & 0 \\ 0 & 0 & 0 & 0 & 0 & 0 & 75 & 0 \\ 0 & 0 & 0 & 0 & 0 & 0 & 0 & -75 \\ 0 & 0 & 22.4 & 0 & -300 & 0 & -150 & 0 \\ 0 & 0 & 0 & -22.4 & 0 & 300 & 0 & -150 \end{bmatrix}, \tag{15}$$

$$B_m = \begin{bmatrix} 0 & 0 & 0 & 0 & 0 & 0 & -1 & 0 \\ 0 & 0 & 0 & 0 & 0 & 0 & 0 & -1 \end{bmatrix}^T, \tag{16}$$

$$C_m = \begin{bmatrix} -2.99 & 0 & -1.19 & 2.46 & -27.64 & 0 & 0 & 0 \\ 0 & -2.99 & 2.46 & 1.19 & 0 & 27.64 & 0 & 0 \end{bmatrix}, \tag{17}$$

The matrix for time-delays is

$$G_d(s) = \begin{bmatrix} e^{-sT_1} & 0 \\ 0 & e^{-sT_2} \end{bmatrix}, \tag{18}$$

where $T_1 = 0.03$ sec and $T_2 = 0.02$ sec. For the controller, the dynamic equations are

$$\dot{X}_c = A_c X_c + B_c e$$
$$\dot{Y}_c = C_c X_c + D_c e \tag{19}$$

where

$$A_c = \begin{bmatrix} 0 & 1 & 0 & 0 \\ 0 & -100 & 0 & 0 \\ 0 & 0 & 0 & 1 \\ 0 & 0 & 0 & -100 \end{bmatrix}, \tag{20}$$

$$B_c = \begin{bmatrix} 0 & 0 \\ 1 & 0 \\ 0 & 0 \\ 0 & 1 \end{bmatrix}, \tag{21}$$

$$C_c = \begin{bmatrix} -12.81 & -21.28 & -463.51 & -30.69 \\ 463.51 & 30.69 & -12.81 & -21.28 \end{bmatrix}, \tag{22}$$

$$D_c = \begin{bmatrix} 0.46 & 0.12 \\ -0.12 & 0.46 \end{bmatrix}. \tag{23}$$

The structure of the autopilot block diagram is shown in Fig. 4. Since the feedback configuration is clearly defined, the GMs and PMs can be analyzed by adding gain-phase-margin testers.

The transfer matrix of the plant is defined by

$$G(s) = C_m(sI - A_m)^{-1} B_m, \tag{24}$$

which gives

$$G(s) = \begin{bmatrix} G_{11}(s) & G_{12}(s) \\ G_{21}(s) & G_{22}(s) \end{bmatrix}, \tag{25}$$

where

$$G_{11}(s) = \frac{-7.657\times10^4 s^5 -1.119\times10^7 s^4 -1.231\times10^8 s^3 +1.674\times10^{11} s^2 +3.575\times10^{12} s +6.810\times10^{14}}{D(s)} \tag{25a}$$

$$G_{12}(s) = \frac{2.073\times10^4 s^6 -3.330\times10^5 s^5 +9.789\times10^7 s^4 +9.368\times10^9 s^3 +1.121\times10^{12} s^2 +3.638\times10^{13} s -2.469\times10^{14}}{D(s)} \tag{25b}$$
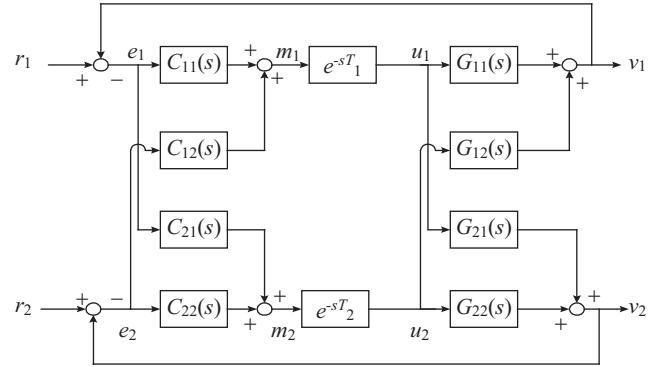

Fig. 4. The structure of block diagram of a missile autopilot system.

$$G_{21}(s) = \frac{2.073\times10^4 s^6 +3.330\times10^5 s^5 +9.756\times10^7 s^4 +9.031\times10^9 s^3 +1.069\times10^{12} s^2 +2.957\times10^{13} s -2.417\times10^{14}}{D(s)} \tag{25c}$$

$$G_{22}(s) = \frac{7.657\times10^4 s^5 +1.119\times10^7 s^4 +1.230\times10^8 s^3 -1.629\times10^{11} s^2 -3.508\times10^{13} s -5.838\times10^{14}}{D(s)} \tag{25d}$$

$$D(s) = s^8 + 3.039\times10^2 s^7 + 6.968\times10^4 s^6$$
$$+ 8.713\times10^6 s^5 + 8.134\times10^8 s^4$$
$$+ 4.153\times10^{10} s^3 + 1.194\times10^{12} s^2$$
$$+ 1.923\times10^{13} s + 2.224\times10^{14}. \tag{25e}$$

The transfer matrix of the controller is defined by

$$C(s) = C_c(sI - A_c)^{-1} B_c + D_c, \tag{26}$$

which gives

$$C(s) = \begin{bmatrix} C_{11}(s) & C_{12}(s) \\ C_{21}(s) & C_{22}(s) \end{bmatrix}$$

$$= \begin{bmatrix} \dfrac{0.46s^2 + 24.72s - 12.81}{s^2 + 100s} & \dfrac{0.12s^2 - 18.69s - 463.51}{s^2 + 100s} \\ \dfrac{-0.12s^2 + 18.69s + 463.51}{s^2 + 100s} & \dfrac{0.46s^2 + 24.72s - 12.81}{s^2 + 100s} \end{bmatrix} \tag{27}$$

1. GMs and PMs of Augmented Open-Loop Transfer Function

From Fig. 4, letting $r_2=0$, one of the augmented open-loop transfer function (AOLTFs) can be obtained; i.e.,

$$g_{01}(s) = \frac{y_1(s)}{e_1(s)}$$

$$= \frac{\begin{aligned}&G_{11}C_{11}e^{-sT_1}(1+G_{22}C_{22}e^{-sT_2}) \\ &+G_{12}C_{21}e^{-sT_2}(1+G_{21}C_{12}e^{-sT_1}) - G_{21}C_{11}G_{12}C_{22}e^{-s(T_1+T_2)} - G_{22}C_{21}G_{11}C_{12}e^{-s(T_1+T_2)}\end{aligned}}{1+G_{22}C_{22}e^{-sT_2} + G_{21}C_{12}e^{-sT_1}}. \tag{28}$$
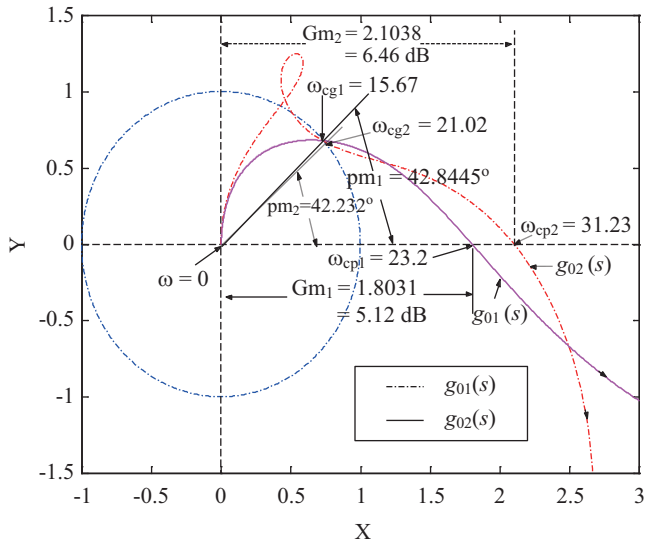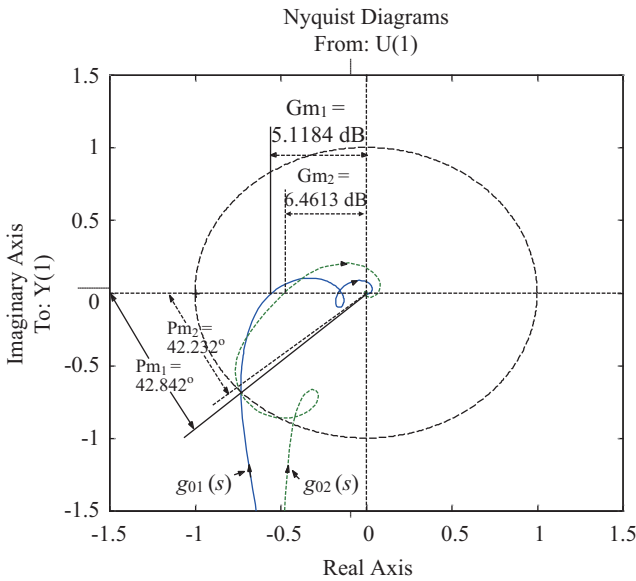
Fig. 5. GMs and PMs for AOLTFs.

Fig. 6. Nyquist plots for checking the results in Fig. 5.

Similarly, letting $r_1 = 0$, the 2nd AOLTF is

$$g_{02}(s) = \frac{y_2(s)}{e_2(s)}$$

$$= \frac{G_{22}C_{22}e^{-sT_2}(1+G_{11}C_{11}e^{-sT_1})}{\substack{+G_{21}C_{12}e^{-sT_1}(1+G_{12}C_{21}e^{-sT_2})-G_{21}C_{11}C_{22}G_{12}e^{-s(T_1+T_2)}-G_{22}C_{21}G_{11}C_{12}e^{-s(T_1+T_2)} \\ 1+G_{11}C_{11}e^{-sT_1}+G_{12}C_{21}e^{-sT_2}}} .$$

(29)

After the gain-phase-margin testers ($A_i\, e^{j\theta_i}$, $i = 1, 2$) are added, the GMs and PMs can be found by use of the X-Y plane method as shown in Fig. 5, in which, the numerical values of GMs, PMs and the cross-over frequencies are indicated. These

results can be checked by use of the Nyquist plots as shown in Fig. 6.

Note that the results shown in Figs. 5 and 6 indicate that both $g_{01}(s)$ and $g_{02}(s)$ have multiple GMs and PMs due to the re-entrant crossings.

2. Single-Block GMs and PMs

After a gain-phase-margin tester ($A_i\, e^{j\theta_i}$) is added, one by one, to all the blocks in Fig. 4 (excepting the two blocks for time-delays), eight different characteristic equations can be found as follows:

$$F_{C11}(s) = [1+G_{22}C_{22}e^{-sT2}+G_{21}C_{22}e^{-sT1}+G_{12}C_{22}e^{-sT2}$$
$$+G_{12}C_{22}C_{22}C_{22}e^{-s(T1+T2)}$$
$$-G_{22}C_{22}G_{22}C_{22}e^{-s(T1+T2)}]$$
$$+Ae^{-j\theta}\cdot[G_{22}C_{22}e^{-sT1}+G_{22}C_{22}G_{22}C_{22}e^{-s(T1+T2)}$$
$$-G_{22}C_{11}G_{22}C_{22}e^{-s(T1+T2)}] = 0,$$

(30)

$$F_{C22}(s) = [1+G_{11}C_{11}e^{-sT1}+G_{21}C_{12}e^{-sT1}$$
$$+G_{12}C_{21}e^{-sT2}+G_{12}C_{21}G_{21}C_{12}e^{-s(T1+T2)}$$
$$-G_{22}C_{21}G_{11}C_{12}e^{-s(T1+T2)}]$$
$$+Ae^{-j\theta}\cdot[G_{22}C_{22}e^{sT2}+G_{11}C_{11}G_{22}C_{22}e^{-s(T1+T2)}$$
$$-G_{21}C_{11}G_{12}C_{22}e^{-s(T1+T2)}] = 0,$$

(31)

$$F_{C12}(s) = [1+G_{11}C_{11}e^{-sT1}+G_{21}C_{12}e^{-sT1}$$
$$+G_{12}C_{21}e^{-sT2}+G_{12}C_{21}G_{21}C_{12}e^{-s(T1+T2)}$$
$$-G_{22}C_{21}G_{11}C_{12}e^{-s(T1+T2)}]$$
$$+Ae^{-j\theta}\cdot[G_{21}C_{12}e^{-sT1}+G_{12}C_{21}G_{21}C_{12}e^{-s(T1+T2)}$$
$$-G_{22}C_{21}G_{11}C_{12}e^{-s(T1+T2)}] = 0,$$

(32)

$$F_{C21}(s) = [1+G_{11}C_{11}e^{-sT1}+G_{22}C_{22}e^{-sT1}$$
$$+G_{21}C_{12}e^{-sT2}+G_{11}C_{11}G_{22}C_{22}e^{-s(T1+T)}$$
$$-G_{21}C_{11}G_{12}C_{22}e^{-s(T1+T2)}]$$
$$+Ae^{-j\theta}\cdot[G_{12}C_{21}e^{-sT2}+G_{12}C_{21}G_{21}C_{12}e^{-s(T1+T2)}$$
$$-G_{22}C_{21}G_{11}C_{12}e^{-s(T1+T2)}] = 0,$$

(33)

$$F_{G11}(s) = [1+G_{22}C_{22}e^{-sT2}+G_{21}C_{12}e^{-sT1}$$
$$+G12C_{21}e^{-sT2}+G_{12}C_{21}G_{21}C_{12}e^{-s(T1+T2)}$$
$$-G_{21}C_{11}G_{12}C_{22}e^{-s(T1+T2)}]$$
$$+Ae^{-j\theta}\cdot[G_{11}C_{11}e-sT1+G_{11}C_{11}G_{22}C_{22}e^{-s(T1+T2)}$$
$$-G_{22}C_{21}G_{11}C_{12}e^{-s(T1+T2)}] = 0,$$

(34)

Fig. 7. GMs and PMs of four controller blocks.

Fig. 8. GMs and PMs of four plant blocks.

$$F_{G22}(s) = [1+G_{11}C_{11}e^{-sT1}+G_{21}C_{12}e^{-sT1}$$
$$+G_{12}C_{21}e^{-sT2}+G_{12}C_{21}G_{21}C_{12}e^{-s(T1+T2)}$$
$$-G_{21}C_{11}G_{12}C_{22}e^{-s(T1+T2)}]$$
$$+Ae^{-j\theta}\cdot[G_{22}C_{22}e-sT2+G_{11}C_{11}G_{22}C_{22}e^{-s(T1+T2)}$$
$$-G_{22}C_{21}G_{11}C_{12}e^{-s(T1+T2)}] = 0, \qquad (35)$$

$$F_{G12}(s) = [1+G_{11}C_{11}e^{-sT1}+G_{22}C_{22}e^{-sT2}$$
$$+G_{21}C_{12}e^{-sT1}+G_{11}C_{11}G_{22}C_{22}e^{-s(T1+T2)}$$
$$-G_{22}C_{21}G_{11}C_{12}e^{-s(T1+T2)}]$$
$$+Ae^{-j\theta}\cdot[G_{12}C_{21}e^{-sT1}+G_{12}C_{21}G_{21}C_{12}e^{-s(T1+T2)}$$
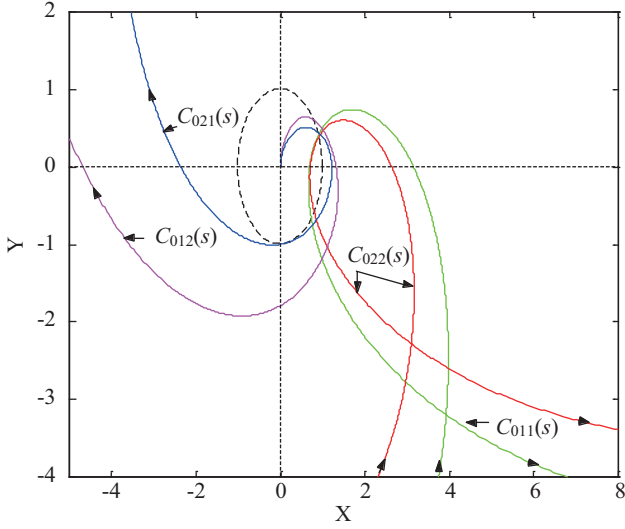$$-G_{21}C_{11}G_{12}C_{22}e^{-s(T1+T2)}] = 0, \qquad (36)$$

Table 1. GMs, PMs and crossover frequencies of four controller blocks.

	ω (rad/sec)	GM, PM
$C_{011}(s)$	$\omega_{cp1} = 21.51$	GM1 = 0.6842 (-3.2963 dB)
	$\omega_{cp1} = 46.77$	GM1 = 3.1471 (9.9582 dB)
	$\omega_{cg1} = 17.22$	PM1 = -42.6446
	$\omega_{cg1} = 25.67$	PM1 = 25.1345
$C_{022}(s)$	$\omega_{cp2} = 21.76$	GM2 = 0.6992 (-3.108 dB)
	$\omega_{cp2} = 40.94$	GM2 = 2.6308 (8.4018 dB)
	$\omega_{cg2} = 18.16$	PM2 = -36.2346
	$\omega_{cg2} = 25.59$	PM2 = 23.5623
$C_{012}(s)$	$\omega_{cp3} = 23.04$	GM3 = 1.3125 (2.362 dB)
	$\omega_{cg3} = 14.99$	PM3 = 37.64
$C_{021}(s)$	$\omega_{cp4} = 22.01$	GM4 = 1.2128 (1.6758 dB)
	$\omega_{cg4} = 15.20$	PM4 = 26.6287
	$\omega_{cg4} = 32.38$	PM4 = -66.4367

Table 2. GMs, PMs and crossover frequencies of four plant blocks.

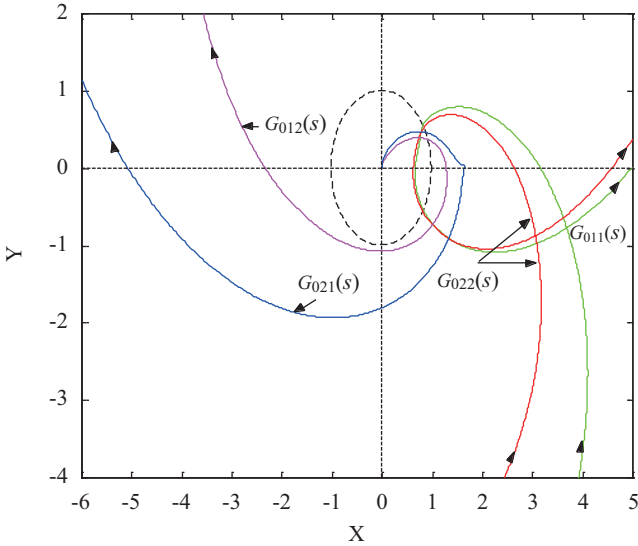|	ω (rad/sec)	GM, PM
$G_{011}(s)$	$\omega_{cp1} = 19.41$	GM1 = 0.6533 (-3.6977 dB)
	$\omega_{cp1} = 46.53$	GM1 = 3.1550 (9.980 dB)
	$\omega_{cg1} = 15.12$	PM1 = -33.9240
	$\omega_{cg1} = 24.77$	PM1 = 35.3112
$G_{022}(s)$	$\omega_{cp2} = 19.72$	GM2 = 0.6148 (-4.225 dB)
	$\omega_{cp2} = 40.90$	GM2 = 2.6283 (8.393 dB)
	$\omega_{cg2} = 15.64$	PM2 = -34.8358
	$\omega_{cg2} = 24.92$	PM2 = 32.8279
$G_{012}(s)$	$\omega_{cp3} = 20.85$	GM3 = 1.2726 (2.0938 dB)
	$\omega_{cg3} = 14.30$	PM3 = 21.7766
$G_{021}(s)$	$\omega_{cp4} = 23.34$	GM4 = 1.6390 (4.2916 dB)
	$\omega_{cg4} = 13.96$	PM4 = 27.7172

$$F_{G21}(s) = [1+G_{11}C_{11}e^{-sT1}+G_{22}C_{22}e^{-sT2}$$
$$+G_{12}C_{21}e^{-sT2}+G_{11}C_{11}G_{22}C_{22}e^{-s(T1+T2)}$$
$$-G_{22}C_{21}G_{11}C_{12}e^{-s(T1+T2)}] \qquad (37)$$
$$+Ae^{-j\theta}\cdot[G_{21}C_{12}e^{-sT1}+G_{12}C_{21}G_{21}C_{12}e^{-s(T1+T2)}$$
$$-G_{21}C_{11}G_{12}C_{22}e^{-s(T1+T2)}] = 0,$$

By use of the X-Y plane method (Tao et al., 1991), the four sets of GMs and PMs of the four controller blocks ($C_{ij}(s)$, $i = 1$, 2; $j = 1$, 2) can be found as shown in Fig. 7. Similarly, the four sets of GMs and PMs of the four blocks in the plant can be found as shown in Fig. 8. Figs. 7 and 8 indicate that some blocks ($C_{011}(s)$, $C_{022}(s)$, $G_{011}(s)$, $G_{022}(s)$) have multiple GMs and PMs, and some blocks ($C_{021}(s)$, $C_{012}(s)$, $G_{021}(s)$, $G_{012}(s)$) have two GMs but one PM. Some of the numerical values of GMs, PMs and cross-over frequencies are given in Tables 1 and 2. All these results have been checked by use of Nyquist plots and computer simulations.
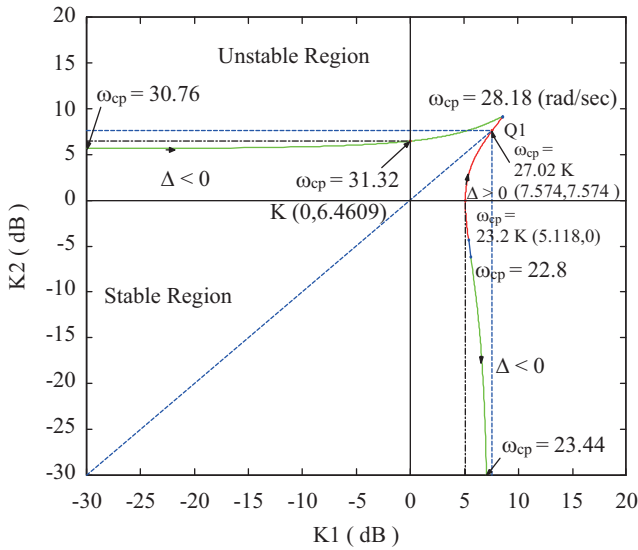
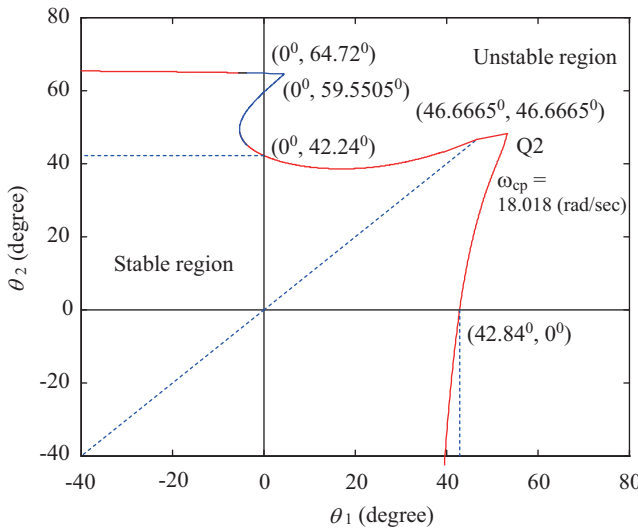**Fig. 9. Stability boundary in the A₁ vs. A₂ plane.**

Fig. 10. Stability boundary in the θ₁ vs. θ₂ plane.

3. Multi-Block GMs and PMs

In Fig. 4, if one tester ($A_1 e^{-j\theta 1}$) is added to blocks $C_{11}(s)$ and $C_{21}(s)$, and another one ($A_2 e^{-j\theta 2}$) is added to blocks $C_{12}(s)$ and $C_{22}(s)$, the system characteristic equation becomes

$$
\begin{aligned}
F(s) = 1 &+ A_1 e^{-j\theta 1} \cdot [G_{11}C_{11}e^{-sT1} + G_{12}C_{21}e^{-sT2}] \\
&+ A_2 e^{-j\theta 2} \cdot [G_{22}C_{22}e^{-sT2} + G_{21}C_{12}e^{-sT1}] \\
&+ A_1 A_2 e^{-j(\theta 1+\theta 2)} \cdot [G_{11}C_{11}G_{22}C_{22}e^{-s(T1+T2)} \\
&+ G_{12}C_{21}G_{21}C_{12}e^{-s(T1+T2)} - G_{22}C_{21}G_{11}C_{12}e^{-s(T1+T2)} \\
&+ G_{21}C_{11}G_{12}C_{22}e^{-s(T1+T2)} = 0,
\end{aligned}
\tag{38}
$$

In order to find the gain-margin, let $\theta_1 = \theta_2 = 0$, $s = j\omega$, and ω is assumed to change from zero to infinity. Then, by use of

the stability-equation method, the stability boundary can be plotted in the A_1 versus A_2 plane as shown in Fig. 9. Assuming that $A_1 = A_2$, point Q_1 indicates that the gain-margin is 7.574 dB, and that the phase cross-over frequency is 27.02 rad/sec.

Similarly, in order to find the phase-margin, let $A_1 = A_2 = 1$, and $s = j\omega$. By changing ω from zero to infinity, the stability boundary can be plotted in a θ_1 vs. θ_2 plane as shown in Fig. 10, where point Q_2 indicates that the phase-margin for $\theta_1 = \theta_2$ is 46.6665°, and that the gain cross-over frequency is 18.018 rad/sec.

From the results given above, it can be seen that, by use of the gain-phase-margin tester method, the GMs and PMs of any single block or any number of blocks can be found easily; thus the method is a useful tool for analyzing the robust characteristics of control systems.

4. A Final Remark

In current literature, the stability conditions of time-delay systems expressed by time-domain models have been analyzed by many authors (Schoen and Geering, 1993; Su, 1995). The relative stability characteristics, such as guaranteed gain-margin and phase-margin, have been extensively studied (Lehtomaki et al., 1981; Zhang and Fu, 1996). From the results presented in this paper, it can be seen that the aforementioned problems can be analyzed more easily by first converting the time-domain models to frequency-domain models (with proper feedback structures), and then adding the gain-phase-margin testers to the system.

V. CONCLUSIONS

The basic definitions and physical meanings of gain-margins (GMs) and phase-margins (PMs) of multi-input multi-output (MIMO) systems have been presented. For those systems originally expressed by time domain models, while converting from state equations to block diagrams, the effects of feedback structures on GMs and PMs have been illustrated. Various GMs and PMs of a missile autopilot system with time-delays have been analyzed. The presented results show that the gain-phase-margin tester method is useful for robust analysis of MIMO systems with time-delays.

REFERENCES

Chang, C. H. and K. W. Han (1989). Gain-margin and phase-margin analysis of a nuclear reactor control system with multiple transport lags. IEEE Trans. on Nuclear Science 36, 1418-1424.

Chang, C. H. and K. W. Han (1990). Gain-margins and phase-margins for control systems with adjustable parameters. AIAA J. of Guidance, Control, and Dynamecs 13, 404-408.

Lehtomaki, N. A., N. R. Sandell and M. Athans Jr. (1986). Robustness results in linear-quadratic Gaussian based multivariable control designs. IEEE Trans. on Automatic Control 26, 75-92.

Li, G. H., C. H. Chang and K. W. Han (1993). Analysis of robust control systems using stability-equations. J. of Control Systems and Technology 1, 83-89.

Li, K. (2013). PID tuning for optimal closed-loop performance with specified

gain and phase margins. IEEE Trans. on Control Systems Technology 21, 1024-1030.

Liceaga-Castro, J. U., E. Liceaga-Castro and I. I. S. Alcala (2012). Phase and gain margins for MIMO linear control systems. Proceeding of the 16th International Conference on System Theory, Control and Computing, Sinaia, Romania, 1-6.

Liu, P. L. (2013). Further results on robust exponential stabilization for time-varying delay saturation actuator systems with delay-dependence. Journal of Marine Science and Technology 21, 127-135.

Liu W. J. (2013). On the stabilization of a class of uncertain systems with time-varying delay via VSC approach. Journal of Marine Science and Technology 21, 508-514.

Paraskevopoulos, P. N., G. D. Pasgianos and K. G. Arvanitis (2006). PID-type controller tuning for unstable first order plus dead time processes based on gain and phase margin specifications. IEEE Trans. on Control Systems Technology 14, 926-936.

Perng J. W., B. F. Wu and T. T. Lee (2006). Limit cycle prediction of a neural vehicle control system with gain-phase margin tester. International Joint Conference on Neural Networks, Vancouver, Canada, 4972-4977.

Postlethwaite, I., J. M. Edmunds and G. J. MacFarlane (1981). Principal gains and principal phases in the analysis of linear multivariable feedback systems. IEEE Trans. on Automatic Control 26, 32-46.

Schoen, G. M. and H. P. Geering (1993). Stability condition for a delay differential system. Int. J. of Control 58, 247-252.

Shenton, A. T. and Z. Shafiei (1994). Relative stability for control systems with sdjustable parameters. AIAA J. of Guidance, Control, and Dynamics 17, 304-310.

Su, J. H. (1995) The asymptotic stability of linear autonomous systems with commensurate time delays. IEEE Trans. on Automatic Control 40, 1114-1117.

Tao, C. S., C. H. Chang and K. W. Han (1991). Gain-margins and phase-margins for multivariable controls systems with adjustable parameters. Int. J. of Control 54, 435-452.

Wang Y. J., S. H. Shih, C. K. Lee, Y. C. Lai and C. M. Chou (2011). Determination of all feasible robust PID controllers for open-loop unstable plus time delay systems with gain margin and phase margin specifications. Proceeding of the 30th Chinese Control Conference, Yantai, China, 2394-2399.

Wang Y. J. (2012). Calculation of all robust PID type controllers for unstable high-order time delay systems based on gain and phase margin specifications. Proceeding of the 31th Chinese Control Conference, Hefei, China, 2775-2780.

Zhang, C. and M. Fu (1996). A revisit to the gain and phase-margins of linear quadratic regulators. IEEE Trans. on Automatic Control 41, 1527-1530.